CERN-TH.6837/93

Hadronic Diffractive Cross Sections and the Rise of the Total Cross Section

Gerhard A. Schuler and Torbjörn Sjöstrand

Theory Division, CERN
CH-1211 Geneva 23
Switzerland

Abstract

A model for high-energy hadronic cross sections is proposed. It is based on Regge theory and perturbative QCD, and includes soft and hard mechanisms as well as diffractive processes. The validity range of Regge-pole theory in the description of total, elastic, single- and double-diffractive cross sections is investigated and inconsistencies found already at LHC/SSC energies. Examining unitarity constraints, modifications of the cross section formulae are proposed which allow a continued use of formulae in the Regge spirit to describe elastic and diffractive events. The non-diffractive cross section is allowed to rise at a rate consistent with unitarization of multiple parton–parton scatterings. However, in our picture, the rise of the total cross section with increasing energy is only partly due to the minijet cross sections; the diffractive topologies rise as well. Fully differential distributions are given and convenient parametrizations derived for the integrated rates of elastic and diffractive events. Predictions for the various partial cross sections at Tevatron, LHC and SSC energies are given and compared to other estimates.

CERN-TH.6837/93
April 1993

1 Introduction

Many approaches have been used to explain the energy variation of the total cross section in hadronic reactions: Regge theory, impact parameter dependence, soft and hard Pomerons, dual topological unitarization, minijets, parton cascading and diffusion, and so on (for a selection of recent work, see refs. [1–14]). These alternative descriptions need not be mutually exclusive, but can represent different aspects of the correct underlying physics, which is still not understood from first principles.

While much effort has gone into the prediction of total and elastic cross sections at future colliders, less has been said about the subdivision of inelastic events into a non-diffractive class, on the one hand, and various diffractive topologies, on the other. Before we can claim a detailed understanding, clearly all partial cross sections must be predictable. Inelastic events have the advantage that distributions are differential in momentum transfers and masses, so that they provide a rich testing ground. Further, knowledge of all components of the total cross section is tightly linked with the study of a number of other interesting physics topics, such as rapidity gaps [15], minijets, hard scattering in diffractive states [16], and heavy flavours.

The ultimate goal is a description of high-energy hadronic interactions that can be derived from the QCD Lagrangian. This is clearly beyond our current capabilities, so instead we try to find an effective description which one day could be related to QCD in some suitable limits. Ideally such a description should be fully consistent, respect s- and t-channel unitarity, and be valid up to infinite energies. However, the simultaneous fulfilment of these requirements can easily lead to a very cumbersome formalism, which may be out of proportion for what is at best an approximation to the true QCD. Our aim in this article is more modest, namely a model that respects basic unitarity constraints but is still practical, i.e. leads to a description of integrated and differential partial cross sections that can easily be confronted with experimental data. At ultra-high energies such a description will cease to be a valid approximation, but we expect this to happen at energies well above those of the next generation of hadron colliders, LHC and SSC.

This paper is divided into three parts. In the first part (section 2) we briefly discuss models of hadronic cross sections in which the rise of the cross section is associated with soft and/or hard Pomerons, in particular Regge theory [17] and 'eikonalized QCD' models [18]. There we also outline the cornerstones of our approach, which combines elements of Regge theory and perturbative QCD. More details of our model are found in the second part (section 3) where we show in some detail the failure of the simple Regge-pole approach and study what minimal modifications could be introduced to save it. Here we also address the rôle of minijets and our model of multiple parton–parton scatterings. The third part of the paper (section 4) is pragmatical: here we use such a modified framework to produce convenient parametrizations of partial (differential and integrated) cross sections for the various event classes, which can then be used to give predictions for current and future colliders. Some final comments are given in section 5.

2 Models of hadronic cross sections

It has long been known that Regge theory leads to a good description of high-energy, low-$|t|$ experimental data [19, 20, 17]. The version of a supercritical Pomeron with $\alpha_{\mathbb{P}}(t) = 1+\epsilon+\alpha' t$, $\epsilon = 0.05$–0.1, $\alpha' = 0.2$–$0.25\,\mathrm{GeV}^{-2}$ describes simultaneously the rising total cross

sections, the $d\sigma/dt$ behaviour of elastic scattering and the phenomenology of diffraction dissociation. A proper unitarization of the theory requires the inclusion of diagrams that describe the interaction of the Pomerons with each other [21–26,13]. These diagrams are ignored in the 'naive' eikonalization, but the theory can be made consistent (fulfil both s- and t-channel unitarity) through inclusion of the so-called enhanced graphs [27] in an extended eikonal [13, 25].

Despite the appeal of such an internally consistent approach, we do not follow it for two reasons, a practical one and a theoretical one.

- The extended-eikonal formalism is well suited to study the energy dependence of integrated cross sections, but does not provide fully differential formulae and final state configurations for all partial cross sections. These distributions *can* be obtained already with a simple, factorizing Pomeron pole (with $\epsilon = \alpha_{I\!P}(0) - 1 > 0$), which gives a good description of the energy dependence of the total cross section, the forward slope B, the ρ-parameter [18] and data on single diffraction [28]. Our aim is therefore to investigate how far the theory of a single supercritical Pomeron ($\epsilon > 0$) can successfully simulate the results of the more complete theory. The great advantage of such a simplification will be the very economical and transparent description of the various diffractive cross sections. Of course, at ultra-high energies such an approach will cease to be a valid approximation.
- Our second argument concerns the nature of the Pomeron. The Pomeron with $\alpha_{I\!P}(0)-1 = \epsilon \approx 0.08$ discussed above is purely phenomenological, i.e. the parameters ϵ and α' are extracted from experimental data. In contrast to this 'soft' Pomeron, the Pomeron that one calculates in perturbative QCD is 'hard' with an intercept close to one-half [29]. It is likely that it leads to an increase of the total cross section as well.

  As long as the soft Pomeron cannot be calculated from QCD[1] or, equivalently, the hard Pomeron cannot uniquely be extrapolated to zero t, the only solution seems to be to add incoherently the contributions from the soft and the hard Pomeron. Indeed, using the eikonal description in impact parameter space [30, 31] reasonable descriptions of total and elastic cross section data can be obtained [18]. Here the eikonal is taken as the sum of a soft ($\propto s^\epsilon$) and a hard component reflecting the soft and the hard Pomeron, respectively. The latter contribution is estimated either as a term $\propto s^J$ with $J \approx 1/2$, or by the perturbative QCD two-two cross sections (minijets) cut at some minimal $p_\perp$.

  However, as already stated, one has to go beyond the naive eikonal for a proper unitarization. How this can be done consistently in a model containing both a soft and a perturbative Pomeron is still an open problem. One might argue that multiparticle t-channel unitarity is not significant at present energies due to the smallness of the triple Pomeron coupling [18]. Then the standard eikonal formalism with inclusion of the triple-Pomeron and Pomeron-loop graphs in first order would provide an implementation of the (larger) s-channel unitarity effects [12].

Here we propose a model in which we do not resort to an explicit unitarization scheme. Rather, corrections to the soft-Pomeron contributions are approximated by using Regge pole theory with a reduced Pomeron intercept. The hard sector, described by the perturbative QCD scatterings is regularized through a model of multiple parton–parton scat-

[1] An attempt to calculate total, elastic and diffraction dissociation cross sections in perturbative QCD without recourse to a soft Pomeron was tried in refs. [9, 14].

terings. The broad outline is as follows, with further details given in subsequent sections.

- Since we do not explicitly unitarize, we cannot predict the rise of the total cross section. Rather we need a $\sigma_{tot}(s)$ parametrization as input to constrain the partial cross sections. We choose the following phenomenological, but elegant and simple description of the total cross section [8]: $\sigma_{tot}(s) = Xs^{\epsilon} + Ys^{-\eta}$. The power $\epsilon = 0.08$ is to be interpreted as an effective one, representing the (combined) increase due to the soft and the hard sectors, and should be expected to have some slow energy dependence.
- Next we model the elastic cross section. The description is based on an *interpretation* of the powerlike increase of $\sigma_{tot} \propto s^{\epsilon}$ as being due to a single-Pomeron pole with $\alpha_{\mathbb{P}}(0) = 1 + \epsilon$. Investigating the s-channel unitarity violation in b-space tells us how to modify the elastic cross section formula so that it still fits existing data but obeys unitarity at high energies.
- Then the inelastic cross section is calculated as the difference between total and elastic ones, and is split into a diffractive and a non-diffractive component. To this end we assume that diffractive processes are dominated by the soft Pomeron. The diffractive cross sections can thus be calculated in Regge-pole theory. Here we choose a critical Pomeron ($\epsilon = 0$) to approximate the unitarity corrections. Then the diffractive cross section will satisfy the Pumplin bound [32] $\sigma_d \leq \frac{1}{2}\sigma_{tot} - \sigma_{el}$.
- Regge theory predicts only the high-mass part of diffractive states. The cross section of the low-mass part is usually taken as a constant times the integrated elastic cross section. Since we are interested in the fully differential cross section formulae, we need a model for the low-mass region in which resonance structures are visible. This is achieved by suitable modifications of the Regge formulae.
- The non-diffractive cross section is finally given by the difference $\sigma_{nd} = \sigma_{tot} - \sigma_{el} - \sigma_d$. At low energies it is solely given by soft-Pomeron contributions, because the perturbative QCD cross section is negligible. As the energy increases, the hard component rises much faster than the soft one. Unitarity corrections will in general mix the various contributions, but we may expect the faster-growing perturbative QCD contribution to dominate at high energies. Allowing for multiple parton–parton scatterings, the unitarized 'minijet' cross section will not grow faster than its upper limit, the non-diffractive cross section.

In the collision of two hadrons A and B, the total cross section is thus subdivided as

$$\sigma_{tot}^{AB}(s) = \sigma_{el}(s) + \sum_{k=1}^{\infty} \sigma_{k\text{-}d}(s) + \sigma_{nd}(s) \ . \tag{1}$$

Here σ_{el} is the elastic scattering $A + B \to A + B$, while $\sigma_{k\text{-}d}$ denotes the cross section of events containing k diffractive subsystems. The dominant diffractive reactions are single diffraction, $A+B \to A+X$ and $A+B \to X+B$, and double diffraction, $A+B \to X_1+X_2$. The non-diffractive event class of σ_{nd} covers the generic process $A + B \to X$, where the system X is supposed not to contain any large rapidity gaps, i.e. to be distinctive from diffractive events. To us, the non-diffractive events are those that involve a net colour exchange between the two incoming hadrons, while diffractive topologies arise from the exchange of colour neutral objects. The experimental samples of diffractive and 'minimum-bias' non-diffractive events are not going to agree exactly with the theoretical definition, with mixing coming e.g. from fluctuations in the fragmentation process and from detector imperfections.

3 A modified Regge description

The exchange of a single, factorizing Pomeron pole leads to the following contribution to the forward scattering amplitude

$$T_{\mathbb{P}}^{AB}(s,t) = \beta_{A\mathbb{P}}(t)\,\beta_{B\mathbb{P}}(t)\,G_{\mathbb{P}}(\xi,t)\ , \tag{2}$$

where $\beta_{A\mathbb{P}}(t)$ denotes the coupling of particle A to the Pomeron. The Green function of the Pomeron, at an 'energy' $\sqrt{s}$ and a 'squared mass' $-t$, is given by

$$G_{\mathbb{P}}(\xi,t) = \xi^{\alpha_{\mathbb{P}}(t)-1}\,\eta\,(\alpha_{\mathbb{P}}) = \xi^{\epsilon}\,e^{\alpha' t\,\ln\xi}\,\eta\,(\alpha_{\mathbb{P}})\ , \qquad \xi = \frac{s}{s_0}\ . \tag{3}$$

Here $\eta\,(\alpha_{\mathbb{P}}) = i - \cot\frac{1}{2}\pi\alpha_{\mathbb{P}}$ $(= i + \rho_{\mathbb{P}}$ for $t = 0)$ is the signature factor, s_0 is a reference scale, and α' is the slope of the Pomeron trajectory, $\alpha_{\mathbb{P}}(t) = \alpha_{\mathbb{P}}(0) + \alpha' t = 1 + \epsilon + \alpha' t$. In the following we will neglect $\rho_{\mathbb{P}}$, which is predicted to be small, in agreement with data. Via the optical theorem the total cross section is

$$\sigma_{tot}^{AB}(s) = \Im T^{AB}(s,0) = \beta_{A\mathbb{P}}(0)\,\beta_{B\mathbb{P}}(0)\,\left(\frac{s}{s_0}\right)^{\epsilon} + Y^{AB}\,s^{-\eta} \equiv X^{AB}\,s^{\epsilon} + Y^{AB}\,s^{-\eta}\ , \tag{4}$$

where the second term arises from ρ, ω, f and a exchange.

Available data on total cross sections are well fitted with [8]

$$\epsilon \approx 0.0808\ , \qquad \eta \approx 0.4525\ . \tag{5}$$

This form very nicely predicts e.g. the Tevatron pp cross section and the HERA γp one. The second term in eq. (4), the Reggeon one, is important only at low energies. From rather low energies onwards, total cross sections are therefore predicted to rise as a single power of the c.m. energy $\sqrt{s}$, $\sigma_{tot} \propto s^{\epsilon}$. Of course, at ultra-high energies unitarity corrections have to become important so that the increase is at most as $\ln^2 s$. But with the above smallness of ϵ, the Froissart–Martin [33] bound is respected up to energies of around 10^{23} GeV [8]. Therefore one might expect reasonable estimates of total cross sections at supercollider energies. In fact, at SSC energies, a pp total cross section of about 120 mb is predicted, well within the range of predictions of other approaches where unitarity is explicitly enforced by using the eikonal formalism, see Table 1.

However, the standard Regge-pole theory with $\epsilon > 0$ leads to inconsistencies in the description of partial cross sections [17]. This is most easily seen when considering the s-channel unitarity condition at low partial waves. The Fourier–Bessel transform

$$f(s,b) = \frac{1}{8\pi^2}\,\int \mathrm{d}^2q\,e^{i\vec{q}\cdot\vec{b}}\,T(s,t) \tag{6}$$

exceeds the unitarity bound $f(s,b) = 1$ for $b = 0$ at about 5 TeV. Here we have taken $s_0 = 1/\alpha'$ and $\alpha' = 0.25\,\mathrm{GeV}^{-2}$ [34]. One might argue that a partial wave analysis is experimentally impossible at such high energies, and thus this violation has no measurable consequences. However, violation of unitarity does show up explicitly. We will demonstrate below that the integrated elastic cross section violates the bound $\sigma_{el}/\sigma_{tot} \leq 1/2$ at about 10^6 GeV. The problem is even more severe for diffractive cross sections: there we find that the single diffractive pp cross section exceeds the total cross section already at around 40 TeV. In fact, higher and higher diffractive production becomes more and

more 'divergent'. Thus, without modifications, the Regge-pole approach cannot be used to predict LHC/SSC partial cross sections.

The elastic cross section is given by $16\pi \mathrm{d}\sigma_{el}^{AB}/\mathrm{d}t = |T^{AB}(s,t)|^2$, so that at high energies, where the Pomeron dominates,

$$16\pi \frac{\mathrm{d}\sigma_{el}^{AB}}{\mathrm{d}t} \stackrel{s\to\infty}{\longrightarrow} \beta_{A\mathbb{P}}^2(t)\, \beta_{B\mathbb{P}}^2(t)\, \left(\frac{s}{s_0}\right)^{2\epsilon}\, e^{2\alpha' t\, \ln\xi}\ . \tag{7}$$

For low t, where the bulk of the cross section is, we can parametrize the form factor for a particle A as $\beta_{A\mathbb{P}}(t) = \beta_{A\mathbb{P}}(0)\exp(b_A t)$. With the s_0 and α' given above, $b_\mathrm{p} \approx 2.3\,\mathrm{GeV}^{-2}$ gives a satisfactory description of pp elastic scattering. Thus the slope parameter B_{el} of standard Regge theory increases logarithmically

$$B_{el}^{AB}(s) = 2b_A + 2b_B + 2\alpha' \ln\left(\frac{s}{s_0}\right)\ , \tag{8}$$

and hence the total elastic cross section rises like $s^{2\epsilon}/\ln s$. As anticipated above, $\sigma_{el}^{\mathrm{pp}}$ exceeds $\frac{1}{2}\sigma_{tot}^{\mathrm{pp}}$ at about $10^3\,\mathrm{TeV}$, the precise value depending on the values of the parameters s_0, α' and b_p.

The Regge-pole model can be made consistent by going to Reggeon field theory. Here we investigate whether we can also obtain 'reasonable' behaviour in the simple Regge-pole model. Inspection of the high-energy limit of eq. (6)

$$f(s,b) \to i\, \frac{\beta_{A\mathbb{P}}(0)\beta_{B\mathbb{P}}(0)}{8\pi} \frac{(s/s_0)^\epsilon}{R^2} \exp\left\{-\frac{b^2}{4R^2}\right\} \tag{9}$$

shows that $f(s,b) \le 1$ can be achieved if the interaction radius R^2 is allowed to rise powerlike ($\propto s^\epsilon$) as well ($R^2 = \frac{1}{2}B_{el}$). The following modification of the Green function of the Pomeron cures the unphysical behaviour of σ_{el}/σ_{tot}

$$G_{\mathbb{P}}(\xi,t) = \left(\frac{s}{s_0}\right)^\epsilon \exp\left\{t\, \left[c_0 \left(\frac{s}{s_0}\right)^\epsilon - c_1\right]\right\}\ . \tag{10}$$

If one takes $c_0 = 2.24\,\mathrm{GeV}^{-2}$ and $c_1 = 2.1\,\mathrm{GeV}^{-2}$, this hardly implies any numerical changes for the energy dependence of $B_{el}(s)$ and $\mathrm{d}\sigma_{el}/\mathrm{d}t|_{t=0}(s)$ in the energy range 10–100 GeV, where the bulk of the data is found (this is the well-known similarity between a log-like behaviour and a behaviour like a small power). For $1.8\,\mathrm{TeV}$ $\overline{\mathrm{p}}\mathrm{p}$ events, the modification gives a change of σ_{el} from 17.0 mb to 14.8 mb. Both numbers are consistent with Tevatron data, $16.6 \pm 1.6\,\mathrm{mb}$ [35].

Asymptotically one obtains a constant ratio σ_{el}/σ_{tot}, because the forward slope is now also increasing power-like

$$B_{el}^{AB}(s) = 2b_A + 2b_B + 2\, \left[c_0 \left(\frac{s}{s_0}\right)^\epsilon - c_1\right]\ . \tag{11}$$

For pp collisions we find that the asymptotic ratio is $\sigma_{el}/\sigma_{tot} = 28\%$. This value is inversely proportional to c_0 (and hence to α'), and could therefore be shifted by some amount. In Table 1 our predictions for LHC and SSC are compared with other estimates, and are found to be in the range of predictions based on eikonal models.

One may ask whether the above modification also guarantees correct asymptotic behaviour of diffractive processes. In the triple-Regge approximation and restricting to

Pomeron exchange, the cross sections of the dominant single and double diffractive processes are

$$16\pi M^2 \frac{\mathrm{d}^2\sigma_{sd}(AB\to AX)}{\mathrm{d}t\,\mathrm{d}M^2} = g_{3\mathbb{P}}(t)\,\beta^2_{A\mathbb{P}}(t)\,\beta_{B\mathbb{P}}(0)\,\left|G_{\mathbb{P}}\left(\frac{s}{M^2},t\right)\right|^2\,\Im G_{\mathbb{P}}\left(\frac{M^2}{s_0},0\right)\ , \quad (12)$$

$$16\pi M_1^2 M_2^2 \frac{\mathrm{d}^3\sigma_{dd}(AB\to X_1X_2)}{\mathrm{d}t\,\mathrm{d}M_1^2\,\mathrm{d}M_2^2} = g^2_{3\mathbb{P}}(t)\,\beta_{A\mathbb{P}}(0)\,\beta_{B\mathbb{P}}(0)\,\left|G_{\mathbb{P}}\left(\frac{ss_0}{M_1^2M_2^2},t\right)\right|^2 \times \Im G_{\mathbb{P}}\left(\frac{M_1^2}{s_0},0\right)\,\Im G_{\mathbb{P}}\left(\frac{M_2^2}{s_0},0\right)\ . \quad (13)$$

Experimental data suggest that the triple-Pomeron vertex $g_{3\mathbb{P}}(t)$ is independent of t and about $0.36\,\mathrm{mb}^{1/2}$ [28]. However, if we do take a constant triple-Pomeron vertex then, even with the modification of eq. (10), σ_{sd} grows faster than σ_{tot}:

$$\frac{\sigma_{sd}}{\sigma_{tot}} \propto \ln\frac{M^2_{max}}{M^2_{min}} \propto \ln s\ . \quad (14)$$

Using the measured ratio $2\sigma^{\mathrm{pp}}_{sd}/\sigma^{\mathrm{pp}}_{tot}$ at fixed target energies [28] one obtains $2\sigma^{\mathrm{pp}}_{sd}/\sigma^{\mathrm{pp}}_{tot} = 1$ already at about 40 TeV.

This inconsistency could be avoided if $g_{3\mathbb{P}}(t)$ vanished at $t = 0$, for example like

$$g_{3\mathbb{P}}(t) = (-t)ge^{at}\ . \quad (15)$$

Then the diffractive cross section in eq. (12) asymptotically grows like the total cross section

$$\frac{2\sigma_{sd}}{\sigma_{tot}} \approx A_1\,\frac{1-(M_0^2/s)^\epsilon}{1+A_2\,(M_0^2/s)^\epsilon}\ . \quad (16)$$

The value of A_2 together with the lower cut-off $M_0^2 \approx 1.5\,\mathrm{GeV}^2$ determine how fast the asymptotic value A_1 is approached. The values for $A_{1,2}$ depend on the parameters assumed, but it is difficult to obtain a 'reasonable' asymptotic ratio. With the above choices ($b_{\mathrm{p}} = 2.3\,\mathrm{GeV}^{-2}$, $c_0 = 2.24\,\mathrm{GeV}^{-2}$, $c_1 = 2.1\,\mathrm{GeV}^{-2}$, $s_0 = 4.0\,\mathrm{GeV}^2$) and taking $a = 2.3\,\mathrm{GeV}^{-2}$ we find $A_1 \approx 60\,\%$ and $A_2 \approx 0.675$. At LHC/SSC energies, the ratio is about 40 %.

More serious than this rather large value is the fact that data do not support $g_{3\mathbb{P}}(0) = 0$. The t distribution of single diffraction is well fitted by an exponential distribution down to the smallest measured values, $|t| = 0.015\,\mathrm{GeV}^{-2}$ [36]. This requires a in eq. (15) to be larger than $60\,\mathrm{GeV}^{-2}$, in contradiction with the measured slope. Therefore, we have to conclude that the modification of eq. (10) does not render Regge theory free of inconsistencies.

This confirms the general observation [17, 22, 24] that corrections to single-pole exchange remain small only if $g_{3\mathbb{P}}(0) = 0$. Even though the absolute magnitude of $g_{3\mathbb{P}}(0)$ is numerically small, the corrections become important already below SSC energies. In the case of single diffraction, the lowest order contribution (described by the triple-Pomeron graph) is screened by the diagram where an additional Pomeron is being exchanged [21]. In b-space this amounts to multiplying $G_{sd}(s,b)$ (where $\sigma_{sd} = \int \mathrm{d}^2b\,G_{sd}(b)$) by the factor $|1-\Im f(s,b)|^2$. This factor goes to zero as $s\to\infty$, thus suppressing pure dissociation in low partial waves ($l \sim \frac{1}{2}b\sqrt{s} \sim \frac{1}{2}\langle R\rangle\sqrt{s}$). For higher diffractive states the corrections become more complicated.

We can try to approximate these corrections by lowering the intercept $\alpha_{\mathbb{P}}(0)$. In particular, if we take $\alpha_{\mathbb{P}}(0) - 1 = 0$ then we make use of the phenomenological success of Regge theory in the description of diffraction up to at least S$\overline{\text{p}}$pS energies [36–40]. It is known that in Regge theory with a critical Pomeron the single-diffractive cross section grows as $\ln \ln s$, and the sum of the diffractive cross sections asymptotically increases power-like with energy

$$\sigma_d = \sum_{k=1}^{\infty} \sigma_{k\text{-}d}(s) \propto s^{\Delta} \ , \tag{17}$$

where $\Delta \approx 0.05$ [17]. The exact value of Δ does depend on model details such as phase space limits, so it would certainly be possible to fine-tune for $\Delta = \epsilon$, i.e. to have a constant ratio σ_d/σ_{tot} asymptotically. However, a value $\Delta < \epsilon$ is not unreasonable either. In any case, the diffractive cross section stays below its upper limit [32], $\frac{1}{2}\sigma_{tot} - \sigma_{el}$.

We have the following picture in mind. Both the soft Pomeron (with a 'bare' intercept $\alpha_{\mathbb{P}}(0) = 1 + \epsilon_{soft} > 1$) and perturbative QCD scatterings contribute to the inelastic cross section, which may be split into diffractive and non-diffractive cross sections. Unitarization will mix soft and hard Pomeron contributions and yield expressions for σ_{tot}, σ_{el} and corrected expressions for σ_d and σ_{nd}. Phenomenologically, it turns out that up to very high energies σ_{tot} is well described by a power-like increase $\sigma_{tot} \propto s^{\epsilon}$ where $\epsilon = 0.08$. Similarly, diffractive cross sections are well described by the Regge formulae with a critical Pomeron. This can be understood if the contribution of the hard Pomeron to diffractive cross sections is negligible. Thus σ_d is predominantly due to contributions from the soft Pomeron which, however, should be taken at a reduced intercept $\epsilon_{eff} < \epsilon_{soft}$ to take into account (at least approximately) the reduction due to the unitarity corrections. In practice, $\epsilon_{eff} = 0$ works well.

In Figs. 1 and 2 we show the partial cross sections σ_i that are obtained under the assumptions on effective ϵ values made above. The latter figure also indicates a possible net contribution from all diffractive topologies.

The non-diffractive cross section can be calculated from $\sigma_{nd} = \sigma_{tot} - \sigma_{el} - \sigma_d$, using our parametrizations of σ_{el} and σ_d. The partial cross sections are shown in Figs. 1 and 2 as functions of the c.m. energy $\sqrt{s}$, and σ_{nd} is found to increase monotonically with $\sqrt{s}$. Since we do not invoke unitarization explicitly, we cannot predict the soft and hard Pomeron contributions to the non-diffractive cross section without an assumption on the energy dependence of $\sigma_{soft} \equiv \sigma_{nd}^{soft}$. We proceed as follows.

Consider first the case of low energies. Then the cross section of QCD parton–parton scatterings (minijets) is negligible compared to the soft Pomeron one for any reasonable lower cut-off $p_{\perp min}$, i.e. $\sigma_{nd} = \sigma_{soft}$. As the energy increases, the minijet cross section sets in. But as long as σ_{hard} is not too large (i.e. for sufficiently small $\sqrt{s}$), the non-diffractive cross section is simply the sum

$$\sigma_{nd}(s) = \sigma_{soft}(s; p_{\perp min}) + \sigma_{hard}(s; p_{\perp min}) \ . \tag{18}$$

At larger energies, the hard cross section rises faster than σ_{nd}, unless $p_{\perp min}$ is made strongly energy-dependent. A strong energy dependence is not sensible, however, because the cut-off should not grow faster than the interaction radius of the proton, i.e. $p_{\perp min}$ should grow only logarithmically (or as s^{ϵ}). The rise of $\sigma_{hard}(s; p_{\perp min})$ is shown in Fig. 3 for two $p_{\perp min}$ choices (see below), one fixed at 1.3 GeV and the other varying according to eq. (19). In either case the rise is faster, at all energies, than that of the non-diffractive

cross section as a whole. Unitarization corrections are supposed to be applied, which then reduce the hard cross section. In our approach, this reduction arises from the allowance of multiple parton–parton scatterings. Because σ_{soft} and σ_{hard} are mixed by the unitarization, the effective soft cross section is reduced as well. Since the increase of the minijet cross section is enough to drive the rise of σ_{nd}, the input σ_{soft} (before unitarization) could well be taken energy-independent.

Our model of non-diffractive events is based on ref. [41]. In this model, $\langle n \rangle = \sigma_{hard}(p_{\perp min})/\sigma_{nd}(s)$ is simply the average number of parton–parton scatterings above $p_{\perp min}$ in an event, and this number may well be larger than unity. In the simplest scenario, interactions at different $p_\perp$ values are assumed to take place independently of each other. This gives a Gaussian distribution in the number of interactions that take place in a given event. In particular, with an average number $\langle n \rangle$ of interactions per event, a fraction $\exp(-\langle n \rangle)$ of events will have no hard interactions at all, and thus be 'true' low-$p_\perp$ ones, with beam jets and nothing else. This simplest unitarization possibility, which gives $\sigma_{soft}(s) = \sigma_{nd}(s) \exp\{-\sigma_{hard}(s; p_{\perp min})/\sigma_{nd}(s)\}$, is also shown in Fig. 3.

In a more sophisticated scenario, interactions are assumed to take place with varying impact parameter. Central collisions are then assumed to lead to enhanced activity, while peripheral ones give reduced activity. While roughly preserving the average behaviour, it is thus possible to increase the fluctuations around this average. The model contains many unknowns; hopefully most of these can effectively be shuffled into the choice of the free parameters of the model, such as $p_{\perp min}$.

The $\mathrm{p}_{\perp min}$ cut-off probably reflects the fact that the incoming hadrons are colour neutral objects: when the $p_\perp$ of an exchanged gluon is made small and the transverse wavelength correspondingly large, the gluon can no longer resolve the individual colour charges, and then the effective coupling is decreased. This mechanism cannot be predicted by perturbative QCD but is also not in contradiction with perturbative QCD calculations, which are always performed assuming scattering of free partons (rather than partons inside hadrons). A first determination of $p_{\perp min}$ was made in ref. [41]. Based on studies of multiplicity distributions in $\overline{\mathrm{p}}\mathrm{p}$ collisions, a value in the range 1.5–2.0 GeV is obtained. For our recent photoproduction study [42], we made a refit to $\overline{\mathrm{p}}\mathrm{p}$ collider data [43], using a modified set of proton structure functions. In order to agree with the average charged multiplicity of minimum bias events one needs $p_{\perp min} \approx 1.3$ GeV at 200 GeV and $p_{\perp min} \approx 1.45$ GeV at 900 GeV. It is not clear whether the difference is significant, but in the following we have taken as extremes either a fix $\mathrm{p}_{\perp min} = 1.3$ GeV or a slow logarithmic variation

$$p_{\perp min} = 1.3 + 0.15 \, \frac{\ln(\sqrt{s}/200)}{\ln(900/200)} \; . \tag{19}$$

4 Parametrizations of partial cross sections

We now specify the details of our model. As parametrization of $\sigma_{tot}(s)$ we take the power-like ansatz of eq. (4) with the parameters given in ref. [8].

The calculation of $\sigma_{el}(s)$ is based on the optical theorem. If one neglects the small real part and assumes a simple exponential fall-off in t, one has $\mathrm{d}\sigma_{el}/\mathrm{d}t = (\sigma_{tot}^2/16\pi) \exp(B_{el} t)$ and $\sigma_{el}(s) = \sigma_{tot}^2(s)/16\pi B_{el}$, where $B_{el} = B_{el}(s)$ is given by eq. (11), with $c_0 = 2.24\,\mathrm{GeV}^{-2}$ and $c_1 = 2.1\,\mathrm{GeV}^{-2}$. (The ρ parameter is about 0.14, i.e. $1 + \rho^2 \approx 1.02$. The non-zero curvature gives a reduction by a factor 0.97 at SSC, using the expected [44] $C = 6$ instead

of the simple-minded $C = 0$. Thus these two neglected effects almost cancel each other, but are anyway both small.)

The single- and double-diffractive cross sections are given by eqs. (12) and (13), with $\epsilon = 0$ in the standard Regge expression of eq. (3). The slope parameters are then

$$B_{sd(AX)} = 2b_A + 2\alpha' \ln\left(\frac{s}{M^2}\right) \ , \tag{20}$$

$$B_{dd} = 2\alpha' \ln\left(\frac{ss_0}{M_1^2 M_2^2}\right) \ , \tag{21}$$

with $b_{\rm p} = 2.3\,\mathrm{GeV}^{-2}$ and $\alpha' = 1/s_0 = 0.25\,\mathrm{GeV}^{-2}$. Single diffraction with the incoming particle A diffractively excited is obtained by trivial substitution $A \leftrightarrow B$. The logarithm in the expressions above could have been replaced by a small power, as we did for elastic scattering, without any significant numerical change in the following.

The Regge formulae for single-, double- and multi-diffraction are supposed to hold in certain asymptotic regions of the total phase space. For example, the single-Regge limit, corresponding to $A + B \to A + X$, needs $|t| \ll M^2 \ll s$. The lower limits of the momentum transfers are generally non-zero, which implies upper limits on the diffractive invariant masses. For $\mathrm{p} + \mathrm{p} \to \mathrm{p} + X$, one has $|t|^{1/2}_{min} \approx m_{\rm p}(M^2 - m_{\rm p}^2)/s$. Requiring $|t| \leq |t|_{cut} \sim m_\pi^2$ implies $M^2 - m_{\rm p}^2 < 0.15s$. Of course, there will be diffraction outside the restrictive regions where the Regge formulae were derived. Lacking a theory which predicts differential cross sections at arbitrary t and M^2 values, we use the Regge formulae everywhere but introduce fudge factors in order to obtain 'sensible' behaviour in the full phase space. These factors are:

$$F_{sd} = \left(1 - \frac{M^2}{s}\right)\left(1 + \frac{c_{res}\, M_{res}^2}{M_{res}^2 + M^2}\right) \ ,$$

$$F_{dd} = \left(1 - \frac{(M_1 + M_2)^2}{s}\right)\left(\frac{s\, m_{\rm p}^2}{s\, m_{\rm p}^2 + M_1^2\, M_2^2}\right)\left(1 + \frac{c_{res}\, M_{res}^2}{M_{res}^2 + M_1^2}\right)\left(1 + \frac{c_{res}\, M_{res}^2}{M_{res}^2 + M_2^2}\right) \ . \tag{22}$$

The first factor in either expression suppresses production close to the kinematical limit. The second factor in F_{dd} suppresses configurations where the two diffractive systems overlap in rapidity space. We modify also the slope of double diffraction

$$B_{dd} = 2\alpha' \ln\left(e^4 + \frac{ss_0}{M_1^2 M_2^2}\right) \ , \tag{23}$$

to keep B_{dd} from becoming smaller than $8\alpha' \approx 2\,\mathrm{GeV}^{-2}$.

In the low-mass region, a resonance structure is visible at low energies for fixed t values [28], while UA4 reports an enhancement by about a factor of two for the contribution from the region $M < 4$ GeV [45]. A detailed modelling of the resonance structure is beyond the scope of the current paper. Instead the last factors in F_{sd} and F_{dd} give a broad enhancement of the production rate in the resonance region up to about $M_{res} = 2$ GeV. The choice of $c_{res} = 2$ gives agreement with the UA4 data. E-710 reports a mass spectrum shape $\mathrm{d}M^2/(M^2)^\alpha$ with $\alpha = 1.13 \pm 0.07$ [46]. Our assumed low-mass enhancement, when smeared with the E-710 mass resolution, corresponds to a shift of an input $\alpha = 1$ distribution to $\alpha \approx 1.05$. In part, the steeper-than-expected mass spectrum can therefore be understood.

The total single- and double-diffractive cross sections are obtained by integrating eqs. (12) and (13) over the full phase space. The result can be parametrized as

$$\begin{aligned}\sigma_{sd}(AB \to AX) &= \frac{g_{3\mathbb{P}}}{16\pi}\,\beta^2_{A\mathbb{P}}(0)\,\beta_{B\mathbb{P}}(0)\,\mathcal{I}_{AX}\ ,\\ \sigma_{dd}(AB \to X_1X_2) &= \frac{g^2_{3\mathbb{P}}}{16\pi}\,\beta_{A\mathbb{P}}(0)\,\beta_{B\mathbb{P}}(0)\,\mathcal{I}_{XX}\ ,\end{aligned} \tag{24}$$

where

$$\begin{aligned}\mathcal{I}_{AX} &= \iint \frac{\mathrm{d}M_X^2}{M_X^2}\,\mathrm{d}t\,F_{sd}\,e^{B_{sd(AX)}t} \approx \frac{1}{2\alpha'}\,\ln\left(\frac{2b_A+2\alpha'\ln(s/M^2_{2min})}{2b_A+2\alpha'\ln(s/M^2_{max,AX})}\right)\\ &\quad+\frac{c_{res}}{2b_A+2\alpha'\ln(s/M_{2res}M_{2min})+B_{AX}}\,\ln\left(1+\frac{M^2_{2res}}{M^2_{2min}}\right)\ ,\\ \mathcal{I}_{XX} &= \iiint \frac{\mathrm{d}M^2_{X1}}{M^2_{X1}}\,\frac{\mathrm{d}M^2_{X2}}{M^2_{X2}}\,\mathrm{d}t\,F_{dd}\,e^{B_{dd}t} \approx \frac{1}{2\alpha'}\,\left((y_0-y_{min})\,\ln\left(\frac{y_0-y_{min}}{e\Delta_0}\right)+\Delta_0\right)\\ &\quad+\frac{c_{res}}{2\alpha'}\ln\left(\frac{\ln(s\,s_0/M^2_{1min}M_{2res}M_{2min})}{\ln(s\,s_0/M^2_{max,XX}M_{2res}M_{2min})}\right)\ln\left(1+\frac{M^2_{2res}}{M^2_{2min}}\right)\ +\ \{1\leftrightarrow 2\}\\ &\quad+\frac{c^2_{res}}{2\alpha'\ln(s\,s_0/M_{1res}M_{1min}M_{2res}M_{2min})+B_{XX}}\,\ln\left(1+\frac{M^2_{1res}}{M^2_{1min}}\right)\ln\left(1+\frac{M^2_{2res}}{M^2_{2min}}\right)\ .\end{aligned} \tag{25}$$

Here $y_0 = \ln(s/m_\mathrm{p}^2)$. The lower mass integration limits $M^2_{1min,2min} = (m_{A,B}+2m_\pi)^2$ and $y_{min} = y_{1min}+y_{2min} = \ln((m_A+2m_\pi)^2/m_\mathrm{p}^2)+\ln((m_B+2m_\pi)^2/m_\mathrm{p}^2)$ are good approximations to where the experimental diffractive mass spectrum turns on [28], while $M_{1res,2res} = m_{A,B}-m_\mathrm{p}+2\,\mathrm{GeV}$ represents the end of the resonance region. An approximate analytical calculation of the integrals gives $M^2_{max,AX} = M^2_{max,XX} = s$, $B_{AX} = B_{XX} = 0$ and $\Delta_0 \approx 2$. The influence of the correct t ranges, the suppression factors and the modified B_{dd} (eq. (23)) may be included by making these parameters energy-dependent functions, with coefficients fitted to the numerical results:

$$\begin{aligned}M^2_{max,AX} &\approx 0.213\,s\ ,\\ B_{AX} &\approx -0.47+\frac{150}{s}\ ,\\ \Delta_0 &\approx 3.2-\frac{9.0}{\ln s}+\frac{17.4}{\ln^2 s}\ ,\\ M^2_{max,XX} &\approx \left(0.070-\frac{0.44}{\ln s}+\frac{1.36}{\ln^2 s}\right)s\ ,\\ B_{XX} &\approx -1.05+\frac{40}{\sqrt{s}}+\frac{8000}{s^2}\ .\end{aligned} \tag{26}$$

These forms can be used roughly from $s = 100\,\mathrm{GeV}^2$ onwards, and give the correct asymptotic behaviour of $\mathcal{I}_{AX}$ and $\mathcal{I}_{XX}$.

Our assumption that diffractive states are generated by a critical Pomeron implies that the $\beta_{A\mathbb{P}}$ coefficients should be defined with $\epsilon = 0$ in eqs. (2) and (3). Since the Pomeron part of the total cross section *is* s-dependent, it is necessary to pick a scale s_1, at which the $\beta_{A\mathbb{P}}$ and $g_{3\mathbb{P}}$ are determined. We have chosen $\sqrt{s_1} \approx 20$ GeV, which is high

enough for diffractive data to be meaningful, but below the region where the total cross section is rising like s^ϵ. For this scale $\sigma_{tot,\mathbb{P}}^{AB} = \beta_{A\mathbb{P}}\beta_{B\mathbb{P}} = X^{AB}s_1^\epsilon$, i.e. (for s in GeV^2)

$$\hat{\beta}_{\mathrm{p}\mathbb{P}} = \beta_{\mathrm{p}\mathbb{P}}\, s_1^{-\epsilon/2} = \sqrt{X^{\mathrm{pp}}} \approx 4.658 \text{ mb}^{1/2} \; . \tag{27}$$

Our fit to data gives $g_{3\mathbb{P}} \approx 0.318$ mb$^{1/2}$. Reinserting this number into eq. (24) and simplifying gives

$$\begin{aligned} \sigma_{sd(AX)}^{AB} &= (0.0336 \text{ mb}^{-1/2}\text{GeV}^{-2})\, X^{AB}\, \hat{\beta}_{A\mathbb{P}}\, \mathcal{I}_{AX} \; , \\ \sigma_{dd}^{AB} &= (0.0084 \text{ GeV}^{-2})\, X^{AB}\, \mathcal{I}_{XX} \; . \end{aligned} \tag{28}$$

At 1.8 TeV this yields $2\sigma_{sd} \approx 10.6$ mb for $M^2/s < 0.05$, which should be compared with the experimental number 9.4 ± 1.4 mb [46]. The predicted energy dependence thus does not seem unreasonable. Further comparisons are given in Table 1.

5 Discussion

The energy dependence of the total and partial pp cross sections is shown in Fig. 1, while the fractional composition is given in Fig. 2. The elastic cross section is seen to approach its asymptotic value (about 28% in case of pp collisions) very slowly. The asymptotic behaviours of the diffractive cross sections are

$$\begin{aligned} \sigma_{sd} &\propto \mathcal{I}_{AX} \propto \ln(\ln s) \; , \\ \sigma_{dd} &\propto \mathcal{I}_{XX} \propto \ln s \, \ln(\ln s) \; . \end{aligned} \tag{29}$$

Hence both diverge when $s \to \infty$, although slower than $\sigma_{tot} \propto s^\epsilon$. The fractions σ_{sd}/σ_{tot} and σ_{dd}/σ_{tot} therefore first increase but later turn over and decrease again. The turnover is at around 100 (300) GeV for single diffraction and at around 5 (50) TeV for double diffraction with (without) the resonance region terms included, but the ratio varies only slowly over a large range of energies. As already mentioned, we believe that a decreasing rate of the simple diffractive topologies discussed so far is compensated by the emergence of more complicated diffractive topologies, i.e. events with more than one rapidity gap. Such events, recently discussed by Bjorken [15], will have rates proportional to higher powers of $\ln s$. At current energies, the total rapidity range is too small to allow significant rates, so one should be able to neglect them. Asymptotically we expect a roughly constant non-zero fraction of diffractive events, as indicated by the envelope in Fig. 2, but with an increasing average number of gaps.

The non-diffractive cross section first falls with energy in the low-energy, Reggeon-dominated region before it starts to rise. The rise of σ_{nd} can be fully accounted for by the onset of minijet production, $\sigma_{hard}(s; p_{\perp min})$. This shows that a consistent unitarization of soft and hard contributions (needed because the latter exceeds σ_{nd} rather quickly, see Fig. 3) is feasible with an energy-independent 'input σ_{soft}' (i.e. σ_{soft} before unitarization). This observation does not fully constrain the details of the unitarization, however. The simplest unitarization possibility in our model, which gives $\sigma_{soft}(s) = \sigma_{nd}(s) \exp\{-\sigma_{hard}(s; p_{\perp min})/\sigma_{nd}(s)\}$, is also shown in Fig. 3.

The $\epsilon = 0$ used for diffractive events should be interpreted as an effective value, after unitarization effects have been taken into account. However, it may well be that diffractive systems of mass M are inherently different from non-diffractive ones at $\sqrt{s} = M$,

specifically that hard scatterings are less important. This could be motivated along the lines of ref. [9], i.e. that screening corrections similar to those that lead to a reduction of diffraction dissociation in the Reggeon calculus [21] will also reduce the contribution due to semihard processes at high energies. It would be in contrast to scenarios in which minijet production in diffraction is estimated using Pomeron structure functions [16, 47], unless the Pomeron structure function does not obey the momentum sum rule or has a low-x behaviour different from hadronic ones. These ideas can and should be tested through measurements of diffractive cross sections at the Tevatron and LHC/SSC: do M^2 and t distributions agree with eqs. (12) and (13), what is the fraction of minijets inside diffraction, are there signs of an anomalously high charm content, etc.?

Finally, we should remind readers that, although we have concentrated on $\mathrm{pp}/\overline{\mathrm{p}}\mathrm{p}$ physics above, the formulae in section 3 should be applicable for any hadron-hadron collision, once the coefficients b_A, X^{AB}, Y^{AB} and $\hat{\beta}_{A\mathbb{P}}$ are given. For instance, for $\pi^+\mathrm{p}$ collisions, $b_\pi \approx 1.4\,\mathrm{GeV}$, the coefficients of ref. [8] and the derived $\hat{\beta}_{\pi\mathbb{P}} = X^{\pi\mathrm{p}}/\sqrt{X^{\mathrm{pp}}} \approx 2.926\ \mathrm{mb}^{1/2}$ give the results shown in Fig. 4. Since the π mass is abnormally light, the ρ mass has been used to define the threshold behaviour: $M_{min} = m_\rho + 2m_\pi$ and $M_{res} = m_\rho - m_\mathrm{p} + 2\,\mathrm{GeV}$.

In conclusion, we re-emphasize the rôle of diffractive cross sections in the rise of the total cross section. It is likely that elastic and diffractive events, on the one hand, and non-diffractive ones, on the other, each give about 50% of the total cross section over a large range of energies, and that the two classes therefore have equally large importance for the rise of the total cross section.

Acknowledgements: We thank P. Kroll, P.V. Landshoff, B. Margolis and M. Ryskin for interesting discussions.

References

[1] J. Pumplin, Phys. Lett. **B289** (1992) 449

[2] B. Block, R. Fletcher, F. Halzen, B. Margolis and P. Valin, Phys. Rev. **D41** (1990) 978;
B. Block, F. Halzen and B. Margolis, Phys. Lett. **B252** (1990) 481

[3] C. Bourrely, J. Soffer and T.T. Wu, Z. Phys. **C37** (1988) 369

[4] M.M. Block and R.N. Cahn, Rev. Mod. Phys. **57** (1985) 563;
M.M. Block and A.R. White, Nucl. Phys. **B** (Proc. Suppl.) **25B** (1992) 59

[5] E. Gotsman, E.M. Levin and U. Maor, DESY 92-040, March 1992

[6] S. Barshay, P. Heiliger and D. Rein, Z. Phys. **C56** (1992) 77

[7] J.R. Cudell and B. Margolis, Phys. Lett. **B297** (1992) 398

[8] A. Donnachie and P.V. Landshoff, Phys. Lett. **B296** (1992) 227

[9] E.M. Levin and M.G. Ryskin, Sov. Phys. Usp. **32** (1989) 479

[10] L. Durand and H. Pi, Phys. Rev. Lett. **58** (1987) 303

[11] A. Capella, J. Tran Thanh Van and J. Kwiecinski, Phys. Rev. Lett. **58** (1987) 2015

[12] P. Aurenche et al., Phys. Rev. **D45** (1992) 92;
R. Engel et al., Phys. Rev. **D46** (1992) 5192;
S. Roesler, R. Engel and J. Ranft, Leipzig preprint UL-HEP-93-01 (1993)

[13] A.B. Kaidalov, L.A. Ponomarev and K.A. Ter-Martirosyan, Sov. J. Nucl. Phys. **44** (1986) 468

[14] M.G. Ryskin and Yu.M. Shabelski, Z. Phys. **C56** (1992) 253

[15] J.D. Bjorken, Phys. Rev. **D47** (1993) 101

[16] G. Ingelman and P.E. Schlein, Phys. Lett. **152B** (1985) 256;
UA8 Collaboration, A. Brandt et al., Phys. Lett. **B297** (1992) 417

[17] P.D.B. Collins, 'An introduction to Regge theory and high energy physics' (Cambridge University Press, 1977), and references therein

[18] For a recent review and references see, e.g., M.M. Block, K. Kang and A.R. White, Int. J. Mod. Phys. **A7** (1992) 4449

[19] P.D.B. Collins, F.D. Gault and A. Martin, Phys. Lett. **47B** (1973) 171

[20] A. Capella and J. Kaplan, Phys. Lett. **52B** (1974) 448

[21] J. Cardy, Nucl. Phys. **B75** (1974) 413

[22] H.D.J. Abarbanel, J.D. Bronzan, R.L. Sugar and A.R. White, Phys. Rep. **C21** (1975) 119

[23] M.S. Dubovikov and K.A. Ter-Martirosyan, Nucl. Phys. **B124** (1977) 163

[24] M. Baker and K.A. Ter-Martirosyan, Phys. Rep. **C28** (1976) 1

[25] H. Cheng and T.T. Wu, 'Expanding Protons: Scattering at High Energies' (M.I.T. Press, Cambridge MA 1987), and references therein

[26] V.A. Abramovskii, E.V. Gedalin, E.G. Gurvich and O.V. Kancheli, 'Inelastic Interactions at High Energies and Chromodynamics' [in Russian], Metsniereba, Tbilisi, 1986, p. 112

[27] V.N. Gribov, Zh. Eksp. Teor. Fiz. **53** (1967) 654 [Sov. Phys.–JETP **26** (1968) 414]

[28] K. Goulianos, Phys. Rep. **101** (1983) 169, and references therein

[29] V.S. Fadin, E.A. Kuraev and L.N. Lipatov, Phys. Lett. **80B** (1975) 50; Zh. Eksp. Teor. Fiz **71** (1976) 840; **72** (1977) 377;
I.I. Balitsky, L.N. Lipatov and V.S. Fadin, in 'Proc. XIV LNPI Winter School' (Leningrad 1979), p. 109;
I.I. Balitsky and L.N. Lipatov, Yad. Fiz. **28** (1978) 1597

[30] T.T. Chou and C.N. Yang, Phys. Rev. Lett. **20** (1968) 1213; Phys. Rev. **170** (1968) 1591; Phys. Rev. **D8** (1973) 2063

[31] H. Cheng and T.T. Wu, Phys. Rev. Lett. **24** (1970) 1456

[32] J. Pumplin, Phys. Rev. **D8** (1973) 2899

[33] M. Froissart, Phys. Rev. **123** (1961) 1053;
A. Martin, Phys. Rev. **124** (1963) 1432

[34] A. Donnachie and P.V. Landshoff, Nucl. Phys. **B267** (1986) 690

[35] E-710 Collaboration, N.A. Amos et al., Phys. Lett. **B243** (1990) 158

[36] Y. Akimov et al., Phys. Rev. Lett. **39** (1977) 1432

[37] Y. Akimov et al., Phys. Rev. **D14** (1976) 3148

[38] CHLM Collaboration, M.G. Albrow et al., Nucl. Phys. **B108** (1976) 1

[39] CHLM Collaboration, J.C.M. Armitage et al., Nucl. Phys. **B194** (1982) 365

[40] UA4 Collaboration, D. Bernard et al., Phys. Lett. **B186** (1987) 227

[41] T. Sjöstrand and M. van Zijl, Phys. Rev. **D36** (1987) 2019

[42] G.A. Schuler and T. Sjöstrand, Phys. Lett. **B300** (1993) 169; CERN-TH.6796/93

[43] UA5 Collaboration, R.E. Ansorge et al., Z. Phys. **C43** (1989) 357

[44] M.M. Block and R.N. Cahn, in '2^{nd} International Workshop on Elastic and Diffractive Scattering', ed. K. Goulianos (Editions Frontières, Gif sur Yvette, 1988), p. 85

[45] UA4 Collaboration, D. Bernard et al., Phys. Lett. **B198** (1987) 583

[46] E-710 Collaboration, N.A. Amos et al., Phys. Lett. **B301** (1993) 313

[47] H. Fritzsch and K.H. Streng , Phys. Lett. **164B** (1985) 391;
E.L. Berger, J.C. Collins, D.E. Soper and G. Sterman, Nucl. Phys. **B286** (1987) 704;
A. Donnachie and P.V. Landshoff, Nucl. Phys. **B303** (1988) 634

[48] N.A. Amos et al., Nucl. Phys. **B262** (1985) 689

[49] UA4 Collaboration, M. Bozzo et al., Phys. Lett. **147B** (1984) 392

[50] E-710 Collaboration, S. Shukla et al., Nucl. Phys. **B** (Proc. Suppl.) **25B** (1992) 11

[51] J. Pumplin, Phys. Lett. **B276** (1992) 517

Table and Figure Captions

Table 1 (Anti-)proton–proton cross sections and forward slope B. The experimental data (at a few representative energies) are taken from a: [48], b: [38], c: [39], d: [49], e: [45], f: [40], g: [50], h: [46]; (the errors in the diffractive cross sections should be enlarged, to take into account the different definitions as well as different integration ranges; most results are for $M^2/s < 0.05$). Model predictions are Goulianos [28] (σ_{tot} from Fig. 40, the rest from eq. (58)), Pumplin [1], BFHMV [2] (extracted from their figures), BSW [3, 51], BCW [4], GLM [5] (models Ω_{IV} and Ω_V), BHR [6], CM [7], DTU [12] (for MRS(D0)), RS [14] (extracted from their figures), KPT [13] (extracted from their figures), SchSj: this work (†total cross sections from [8]; single diffractive cross section within the experimental cuts, $M^2/s < 0.05$, in parentheses).

Fig. 1 The total pp cross section $\sigma_{tot}^{\rm pp}(s)$, top full curve. The different components are separated by dashed lines, from bottom to top elastic, single diffractive (pX and Xp, equally large but shown separately), double diffractive, and non-diffractive.

Fig. 2 Fractional cross sections $\sigma_i^{\rm pp}(s)/\sigma_{tot}^{\rm pp}(s)$. Dash-dotted elastic, dashed single and double diffractive, dotted the sum of single and double diffraction and the (assumed) envelope of diffraction, and full the non-diffractive fraction.

Fig. 3 The subdivision of the non-diffractive pp cross section: $\sigma_{nd}(s)$ full curve, non-unitarized $\sigma_{hard}(s; p_{\perp min})$ dashed (for two alternative $p_{\perp min}$ choices), and unitarized $\sigma_{soft}(s; p_{\perp min}) = \sigma_{nd}\, \exp(-\langle n \rangle)$ dash-dotted (same two alternatives).

Fig. 4 The total and partial cross sections for π^+p scattering. Notation as in Fig. 1, with the π^+X diffractive cross section below the Xp one.

	σ_{tot} [mb]	σ_{el} [mb]	B_{el} [GeV^{-2}]	$2\sigma_{sd}$ [mb]	σ_{dd} [mb]
pp at $\sqrt{s} = 23.5$ GeV					
Exp.	39.20 ± 0.13^a	6.81 ± 0.19^a	11.80 ± 0.30^a	6.07 ± 0.17^b	–
SchSj	$39.36^\dagger$	6.79	11.66	7.09 (5.09)	1.90
Goulianos	40	7.1	–	5.8	1.6
pp at $\sqrt{s} = 62.5$ GeV					
Exp.	43.51 ± 0.16^a	7.51 ± 0.19^a	13.02 ± 0.27^a	7.5 ± 0.3^c	–
SchSj	$43.66^\dagger$	7.61	12.80	8.52 (6.72)	3.08
Goulianos	44	7.7	–	8.2	2.9
$\overline{\rm p}$p at $\sqrt{s} = 546$ GeV					
Exp.	61.9 ± 1.5^d	13.3 ± 0.6^d	15.5 ± 0.8^e	9.4 ± 0.7^f	–
SchSj	$60.42^\dagger$	11.60	16.08	11.13 (9.36)	5.73
Goulianos	57	10.0	–	14.0	6.5
Pumplin	62.1	–	16.7	6.8–14.2	–
DTU	60	10	–	8.7	–
$\overline{\rm p}$p at $\sqrt{s} = 1800$ GeV					
Exp.	72.8 ± 3.1^g	16.6 ± 1.6^h	16.99 ± 0.47^g	9.4 ± 1.4^h	–
SchSj	$72.98^\dagger$	14.76	18.43	12.38 (10.60)	7.30
Goulianos	63	11.0	–	17.3	9.0
BHR	76.1	17.6	17.2	12.0	–
Pumplin	72.7–73.1	–	17.7	7.6–16.6	–
DTU	71	13	–	9.6	–
pp at $\sqrt{s} = 16$ TeV					
SchSj	$103.72^\dagger$	22.80	24.12	14.41 (12.64)	10.41
Goulianos	74	13.0	–	23.2	13.8
Pumplin	92.3–94.6	–	19.2–19.7	9.0–20.4	–
BFHMV	108	31	19.5	–	–
BCW	105	22.9–28.4	20.0–24.8	–	–
DTU	96	21	–	10.6	–
RS	108	32	–	6.7	6.5
pp at $\sqrt{s} = 40$ TeV					
SchSj	$120.27^\dagger$	27.21	27.17	15.19 (13.42)	11.80
Goulianos	82	14.4	–	25.7	15.3
Pumplin	100.7–104.1	–	20.0–20.7	9.4–21.8	–
BFHMV	121	36.5	20.7	–	–
BSW	121.2	36.4	21.1	–	–
BCW	118	25.9–33.4	21.5–27.7	–	–
GLM	134–191	40–63	21–57	–	–
BHR	144.1	42.6	25.7	13.9	–
CM	140–230	–	–	–	–
DTU	109	26	–	11.0	–
RS	133	42	–	7.2	4.9
KPT	111	27	–	24	–

Table 1

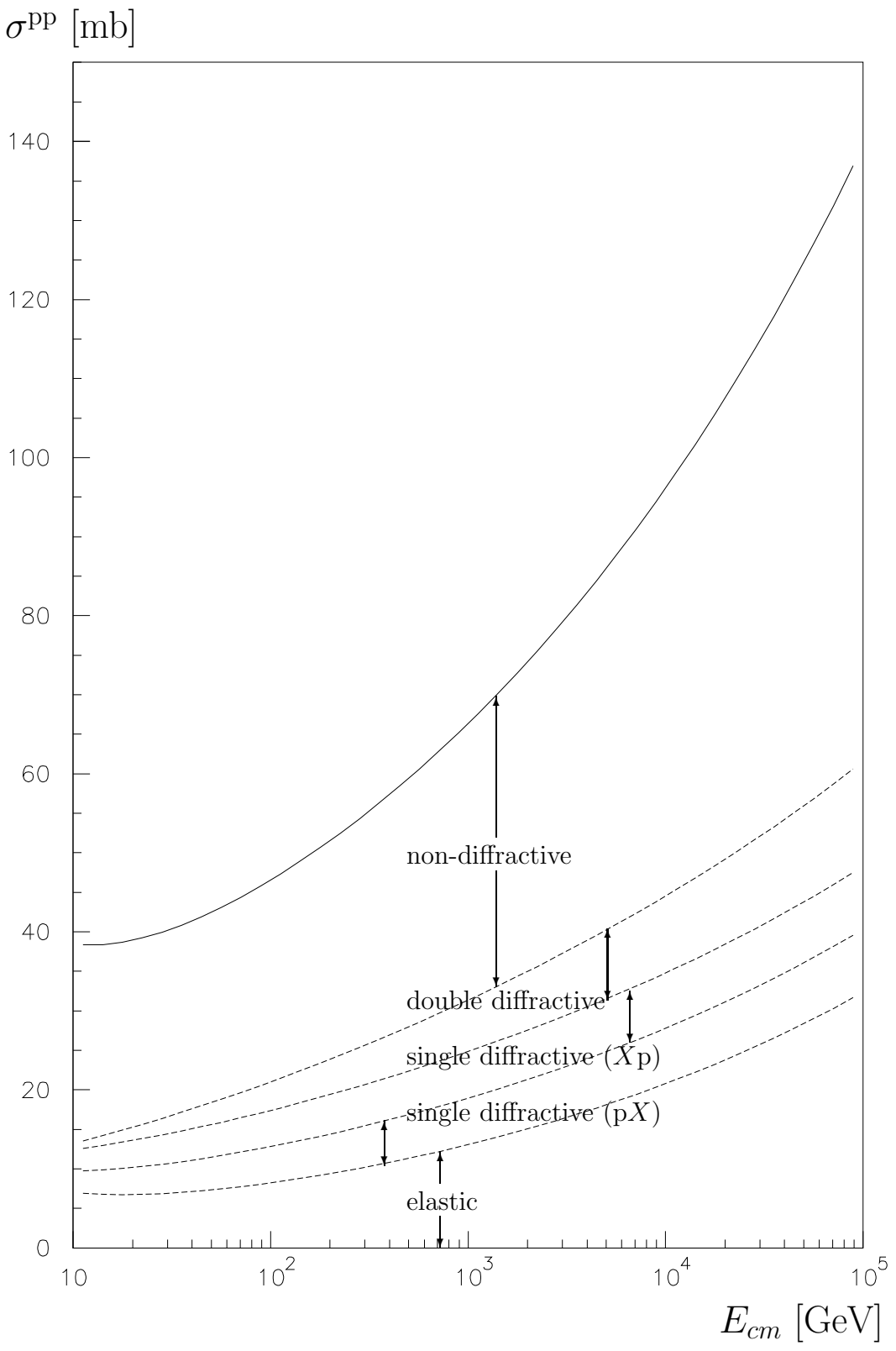
σ^{pp} [mb]
140
120
100
80
60
40
20
0
10
10^2
10^3
10^4
10^5
E_{cm} [GeV]
non-diffractive
double diffractive
single diffractive (Xp)
single diffractive (pX)
elastic

Fig. 1

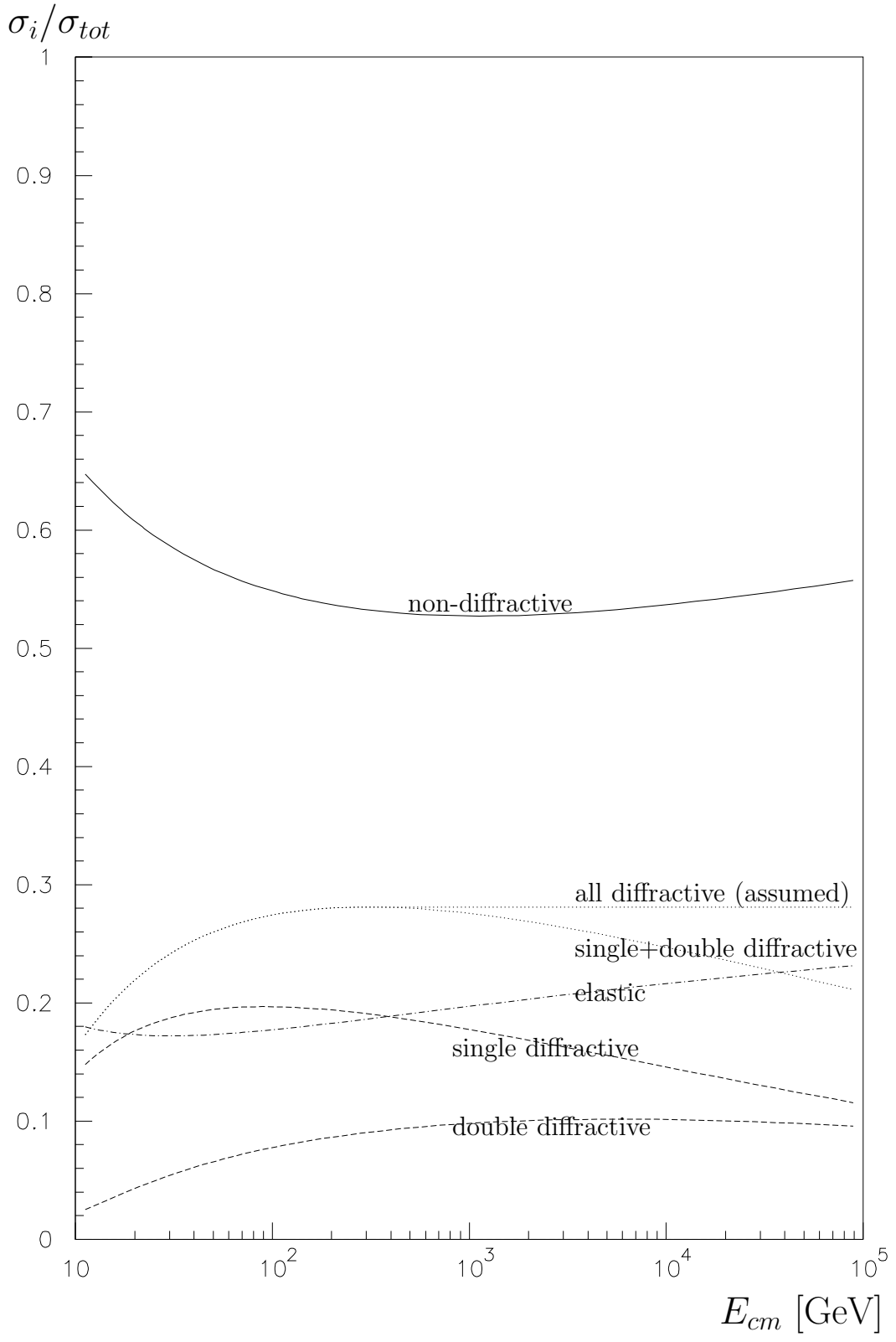
σ_i/σ_{tot}
1
0.9
0.8
0.7
0.6
0.5
0.4
0.3
0.2
0.1
0
non-diffractive
all diffractive (assumed)
single+double diffractive
elastic
single diffractive
double diffractive
10
10^2
10^3
10^4
10^5
E_{cm} [GeV]

Fig. 2

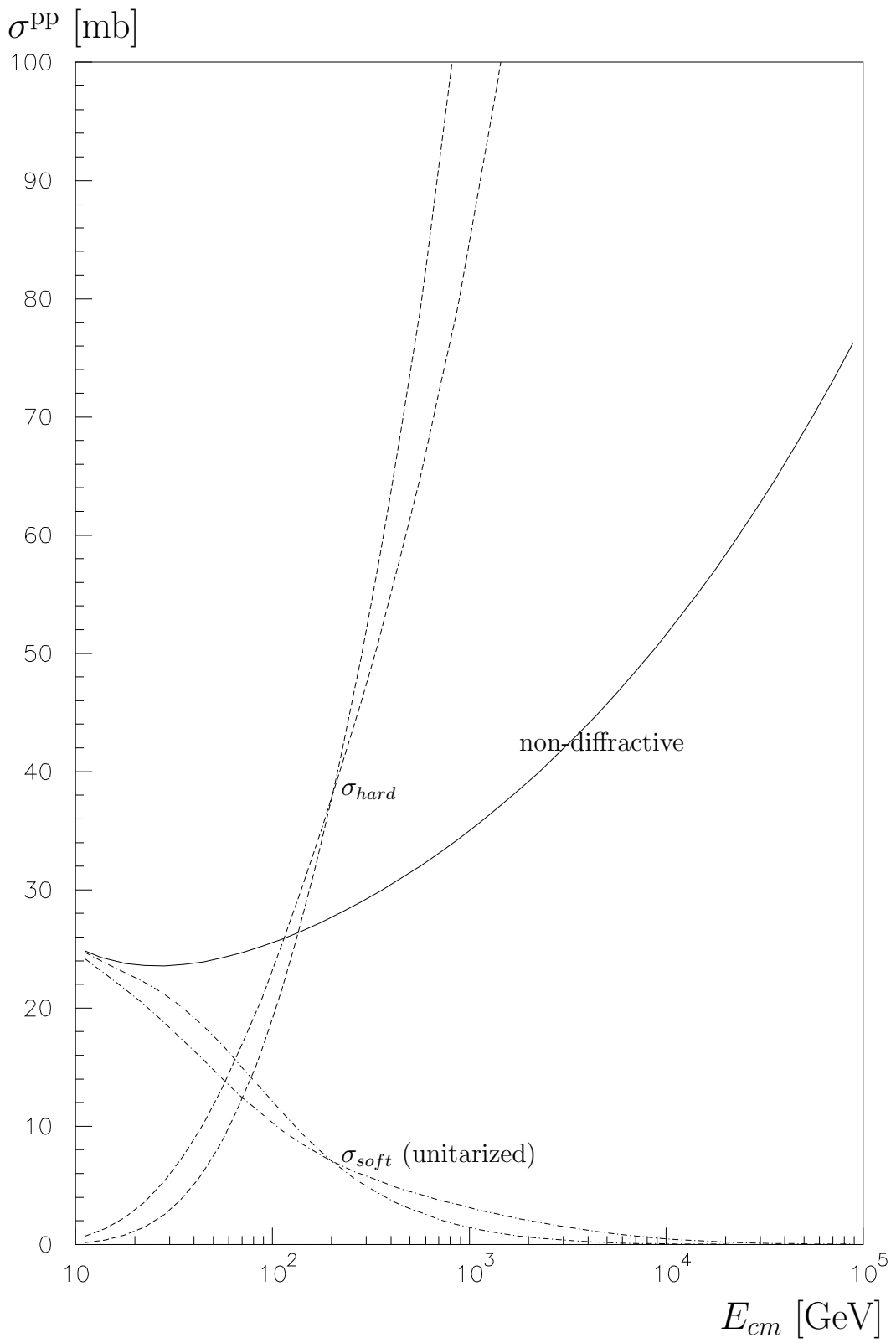
σ^{pp} [mb]
100
90
80
70
60
50
40
30
20
10
0
10
10^2
10^3
10^4
10^5
E_{cm} [GeV]
non-diffractive
σ_{hard}
σ_{soft} (unitarized)

Fig. 3

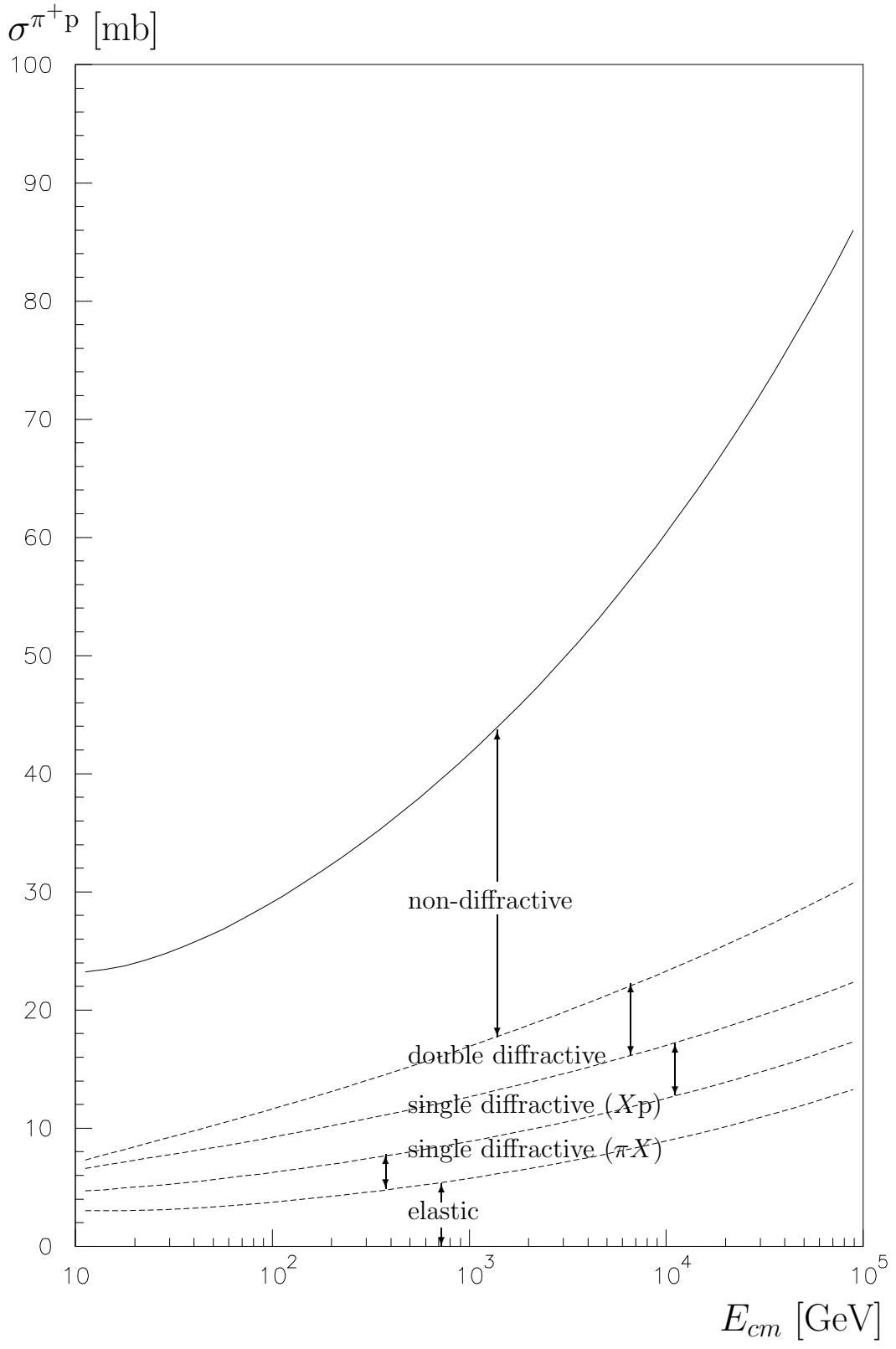
$\sigma^{\pi^+ \mathrm{p}}$ [mb]
100
90
80
70
60
50
40
30
20
10
0
non-diffractive
double diffractive
single diffractive (Xp)
single diffractive (πX)
elastic
10
10^2
10^3
10^4
10^5
E_{cm} [GeV]

Fig. 4